ACOUSTICS 2017 PERTH
SOUND, SCIENCE AND SOCIETY

Airgun arrays for marine seismic surveys - physics and directional characteristics

Alec J Duncan

Centre for Marine Science and Technology, Curtin University, Perth, Australia

ABSTRACT

Airgun arrays are by far the most commonly used offshore seismic survey sound sources and, despite ongoing attempts to develop alternatives, are likely to remain so well into the future. Although designed to produce their highest sound levels in the vertically downward direction, these arrays also emit considerable acoustic energy in other directions, thus making them a potential hazard for marine animals. Each airgun array produces a complicated sound field, determined by the array layout (positions and sizes of its airguns), in which both the waveform and spectrum of the signal vary strongly with direction. This paper examines the relationship between the array layout and the directional characteristics of the sound field it produces with a view to providing guidance on how changes in array layout can be used to reduce the environmental impact of an array while retaining its utility as a seismic survey source.

1 INTRODUCTION

The search for oil and gas reserves using marine seismic surveys involves the use of intense, low-frequency sound to image the geological structure of the seabed. The sound sources are designed to maximise their output in the vertically downward direction in order to maximise the distance into the seabed at which images can be obtained, however considerable acoustic energy is also radiated horizontally into the water column, where it becomes a potential hazard for marine life. This has been an issue of some concern for several decades now, and a number of studies have attempted to quantify the sound levels at which various impacts may occur, mainly in the context of possible impacts on marine mammals (see, for example, Compton et. al 2008; Gisiner, 2016; Southall et. al., 2007). More recently, there has been concern about the possible impact of the high sound levels at the seabed directly under a seismic source in shallow water on site-attached species that are unable to move out of the way of the approaching source (McCauley et. al., 2003; McCauley et. al., 2017). In this case the main concern relates to commercial species of crustaceans and some site attached species of fish.

By far the most common sound source used for marine seismic surveys is the airgun array (Parkes and Hatton, 1986), and despite the active development of alternatives based on various forms of marine vibrators (PGS, 2005; Tenghamn, 2006; LGL and MAI.,2011, Duncan et. al. 2017) this is likely to remain the case well into the future. Although there are a number of variations, the most common form of airgun array consists of a horizontal, planar array of individual airguns of different sizes. Fig. 1 shows a schematic plan view of an array typical of those used for 3D seismic surveys. The number of airguns in an array may be anything up to 40 or so, depending on the nature of the survey.

Each airgun consists of a cylinder of compressed air at high pressure (usually about 14 MPa). The air is suddenly released into the water in response to an electrical trigger signal, resulting in an acoustic signal consisting of an initial high-amplitude pressure pulse followed by a decaying series of “bubble pulses” formed by oscillations of the resulting air bubble (Fig. 2).

For logistical reasons, airgun arrays are usually made up of a small number of parallel subarrays, each of which contains a larger number of airguns. For example, the array shown in Fig. 1 has three subarrays, each containing 7 to 10 airguns.

For the purposes of the seismic survey, the initial pressure pulse is desirable, but the oscillating bubble pulses are not, so various techniques are used to reduce the influence of the bubble pulses. The interval between bubble pulses increases with increasing gun volume, therefore airguns of different sizes are usually used in an array so that when the airguns are simultaneously fired their initial pressure pulses add constructively whereas their bubble pulses tend to cancel out. Another common technique is to use closely spaced pairs of airguns known as clusters,

in which the interaction between the expanding bubbles of the adjacent airguns increases the rate of energy loss and hence the bubble damping.

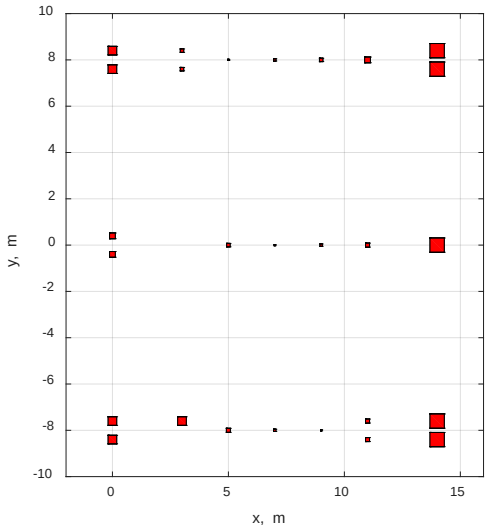

Figure 1: Plan view of a typical medium sized seismic survey airgun array with a total compressed air volume of 49.2 l (3000 cui). The symbols represent the individual airguns and their linear dimensions are proportional to those of the corresponding airguns' air chambers.

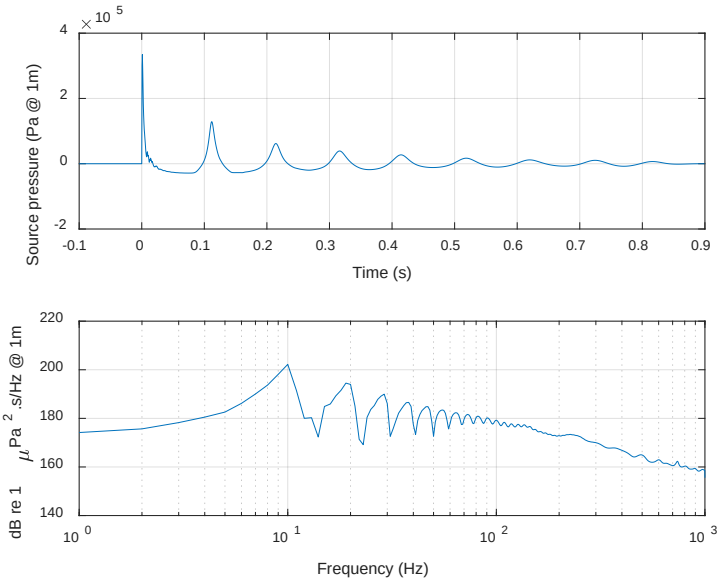

Figure 2: Modelled waveform (top) and spectrum (bottom) of a typical airgun.

This paper focuses on the effect that the layout of the airguns in an array has on its acoustic output, particularly for the elevation angles close to the horizontal that are important for sound levels in the water column at horizontal ranges that are large compared to the dimensions of the array. The results obtained are therefore of most relevance to considerations of behavioural impacts on marine animals, which are usually quantified by the sound exposure level (SEL), which is the decibel representation of the integrated squared pressure, and is a measure of the energy of the acoustic signal (Southall et. al., 2007).

Section 2 of this paper presents a theoretical framework that can be used to calculate the acoustic output in any direction from an arbitrary array of sources. In Section 3 this framework is applied to a number of highly simplified scenarios that nonetheless provide useful insights, and relates these to numerical model calculations of the acoustic characteristics of a realistic airgun array. Section 4 discusses the implications of these results for the design of airgun arrays that minimise their environmental impact. Finally, section 5 summarises the main conclusions from this work.

2 THEORY

The geometry for calculating the contribution of airgun m at position $\boldsymbol{r}_m$to the received signal at position $\boldsymbol{r}$ is shown in Fig. 3. The vector $\hat{\boldsymbol{r}} = \boldsymbol{r}/r$, is a unit vector in the direction from the origin to the receiver, where $r = |\boldsymbol{r}|$, and $\boldsymbol{d}_m$ is the position vector of the receiver relative to airgun m.

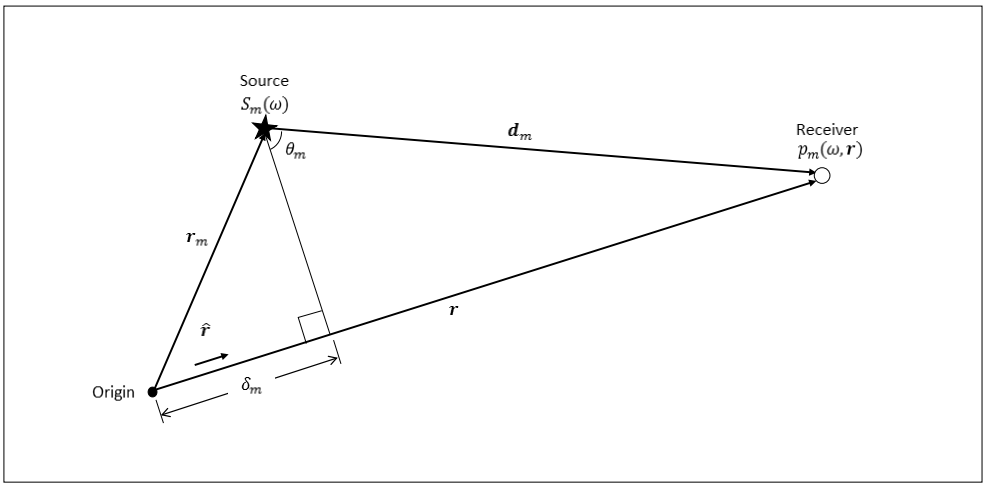

Figure 3: Geometry for calculation of array output

The signal emitted by the airgun is defined by $p_{0,m}(\omega)$, which is the Fourier transform of the far-field source waveform, and $\omega = 2\pi f$ is the angular frequency. Here the term "far-field source waveform" is used to mean the acoustic pressure waveform at a reference distance d_0 (usually taken as 1 m) from an equivalent point source, and the term "equivalent point source" means an ideal point source that would produce the same acoustic field as the real source at ranges much larger than the dimensions of the real source. Because the array consists of airguns of a variety of sizes, $p_{0,m}(\omega)$ will be different for different airguns.

Modelling each airgun as an omnidirectional point source (a good assumption because the airgun bubble is small compared to the acoustic wavelength for frequencies up to several kHz), and assuming an $e^{-i\omega t}$ time dependence, the acoustic pressure signal received at $\boldsymbol{r}$ due to airgun m in an infinite homogeneous medium is:

$$p_m(\omega, \boldsymbol{r}) = \frac{d_0 p_{0,m}(\omega) e^{ik(d_m - d_0)}}{d_m} \tag{1}$$

where $k = \omega/c$ is the acoustic wavenumber, c is the sound speed, and $d_m = |\boldsymbol{d}_m|$ is the distance of the receiver from the airgun.

For a receiver in the far-field of the array, (i.e. $r \gg r_m$), $\boldsymbol{d}_m$ and $\boldsymbol{r}$ are effectively parallel, so θ_m is a right-angle, and $d_m = r - \delta_m$ where δ_m is the component of $\boldsymbol{r}_m$ in the direction of $\boldsymbol{r}$, i.e. $\delta_m = \boldsymbol{r}_m \cdot \hat{\boldsymbol{r}}$. Substituting for d_m in Equation (1) gives

$$p_m(\omega, \boldsymbol{r}) \approx \frac{d_0 p_{0,m}(\omega) e^{ik(r - \boldsymbol{r}_m \cdot \hat{\boldsymbol{r}} - d_0)}}{r} \tag{2}$$

Here the approximation $d_m - d_0 = r - \delta_m - d_0 \approx r$ has been used to simplify the denominator, but this approximation cannot be used in the numerator because of the sensitivity of the phase of the complex exponential to small changes in its argument.

The signal received at $\boldsymbol{r}$ due to the entire array can then be obtained by summing Equation (2) over the M airguns in the array:

$$p(\omega, \boldsymbol{r}) \approx \sum_{m=1}^{M} \frac{d_0 p_{0,m}(\omega) e^{ik(r - \boldsymbol{r}_m \cdot \hat{\boldsymbol{r}} - d_0)}}{r} = \frac{d_0 e^{ik(r-d_0)}}{r} \sum_{m=1}^{M} p_{0,m}(\omega) e^{-ik\boldsymbol{r}_m \cdot \hat{\boldsymbol{r}}} \tag{3}$$

Equation (3) can also be written:

$$p(\omega, \boldsymbol{r}) \approx \frac{d_0 e^{ik(r-d_0)}}{r} \sum_{m=1}^{M} p_{0,m}(\omega) e^{-ik(x_m \hat{x} + y_m \hat{y} + z_m \hat{z})} \tag{4}$$

where $\boldsymbol{r}_m = (x_m, y_m, z_m)$, and $\hat{\boldsymbol{r}} = (\hat{x}, \hat{y}, \hat{z})$. Here $\hat{x}$ etc. can be recognised as the direction cosines of the receiver position relative to the coordinate system origin.

It is often convenient to consider the far-field source spectrum of the array in the direction of the receiver, which is obtained by putting $r = d_0$ in Equation (4), giving:

$$p_0(\omega) \approx \sum_{m=1}^{M} p_{0,m}(\omega) e^{-ik(x_m \hat{x} + y_m \hat{y} + z_m \hat{z})} \tag{5}$$

This should be interpreted as the spectrum of the acoustic pressure signal in the direction of the receiver, 1 m from an equivalent point source.

3 APPLICATION TO EXAMPLE SCENARIOS

3.1 Linear array of sources

It is instructive to consider the simple case of a linear array of sources aligned with one of the coordinate system axes. For example, for an array of sources along the Y-axis, $x_m = z_m = 0$, and Equation (5) becomes:

$$p_0(\omega, \theta) \approx \sum_{m=1}^{M} p_{0,m}(\omega) e^{-iky_m \hat{y}} \tag{6}$$

In this case, for a given array (fixed values of x_m), the argument of the exponential depends only on $k\hat{y} = \frac{\omega}{c} \sin\theta$, where θ is the angle between the direction to the source and the X-axis. $k\hat{y}$ can also be recognised as the Y component of the wave vector of the acoustic wave propagating towards the receiver, and can be varied by changing either the signal frequency or the direction of the receiver. Equation (6) can therefore be used to calculate the beam pattern of the array at a fixed frequency or the spectrum of the signal in a fixed direction.

Fig. 4 plots $20 \log_{10}|p_0|$ against $k\hat{y}$ for the case of $p_{0,m}(\omega) = 1/M$, with the number of sources, M, ranging from 1 to 5 (i.e. each source in a given array has a flat spectrum with an amplitude equal to the inverse of the number of sources in the array). Except for the $M = 1$ case, the overall length of the array is 16 m and the sound speed is 1500 ms^{-1}. The theoretical result for a 16 m long continuous line source (Kinsler et. al., 2000) is also shown for comparison.

With this scaling, all arrays have a relative response of 0 dB at $k\hat{y} = 0$, which corresponds to broadside incidence ($\theta = 0$) at all frequencies, and also corresponds to zero frequency in all directions. The width of the $k\hat{y} = 0$ peak increases slightly with increasing numbers of sources and asymptotes to the continuous line source result as $M \rightarrow \infty$.

The result for a single source ($M = 1$) is independent of $k\hat{y}$, as expected for an omnidirectional point source with a flat spectrum. There are two distinct types of peaks visible in the results for the other arrays: those that reach a maximum of 0 dB, which are known as grating lobes, and those that have lower amplitude peaks, which are

known as sidelobes. From Fig. 4 it is apparent that, as the number of sources increases, the spacings between the grating lobes increase and the amplitudes of the sidelobes decrease.

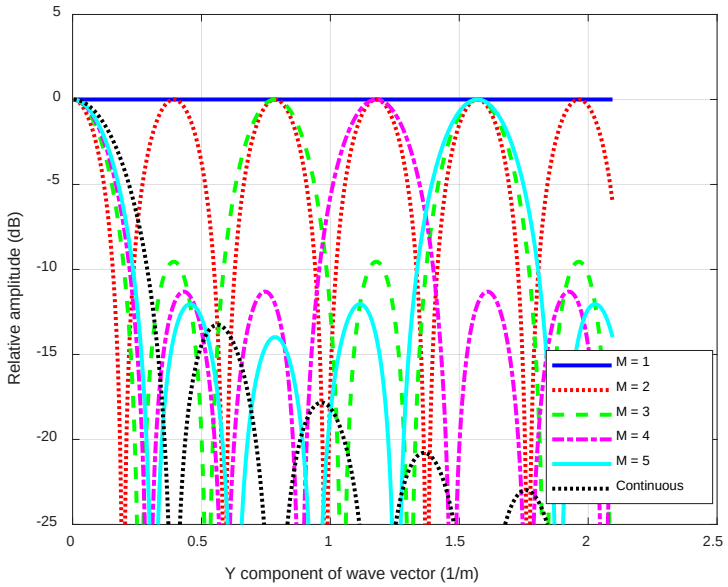

Figure 4: Far-field source spectra as a function of $k\hat{y}$ for the five linear arrays described in the text and the theoretical beam pattern of a continuous line source of the same length (Kinsler et. al., 2000).

The first grating lobe occurs when the signals from each source arrive at the receiver with successive phase shifts of 2π, which corresponds to the condition that $k\hat{y}\delta = 2\pi$, where δ is the distance between sources. In the Y direction ($\theta = 90°$) this corresponds to the frequency at which the acoustic wavelength equals the source spacing, or $f = c/\delta$.

Alternatively, the results from Equation (6) can be plotted as a function of both frequency and angle. A polar plot of this type for the $M = 3$ array is shown in Fig. 5. In this plot, moving out from the origin along a radial gives the spectrum of the signal in that direction, and the 90° spectrum corresponds to the same range of $k\hat{y}$ values as Fig. 4. The geometry of the plot is such that $f \sin\theta$, and hence $k\hat{y}$, is constant along any horizontal line, leading to the distinctive pattern of horizontal stripes.

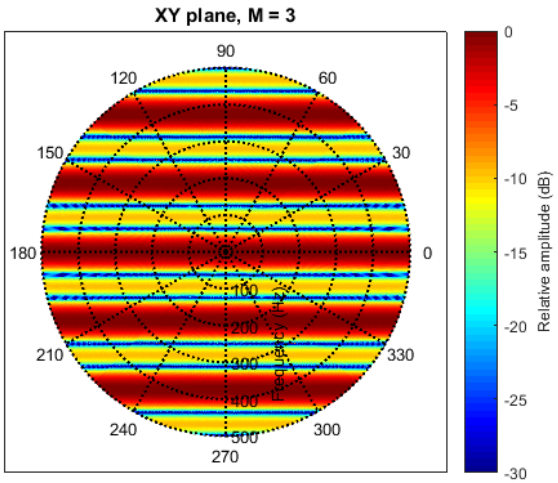

Figure 5: Far-field source output ($20\log_{10}|p_0|$) plotted as a function of both frequency (radial coordinate) and angle from the X axis for the three-source array.

The results shown so far are for arrays consisting of sources with identical, flat spectra. As shown in Fig. 2, the output of a real airgun array decreases with increasing frequency above the bubble pulse frequency. Approximating this as a spectrum that is flat to 10 Hz and then drops off at 20 dB per decade above this, results in Fig. 6.

The grating lobes are still clearly visible but their amplitudes now reduce with increasing frequency. Therefore the first grating lobe of an array with a small number of sources will have a higher amplitude than that of an array with a larger number of sources because of the lower frequency at which the first grating lobe of the smaller array occurs.

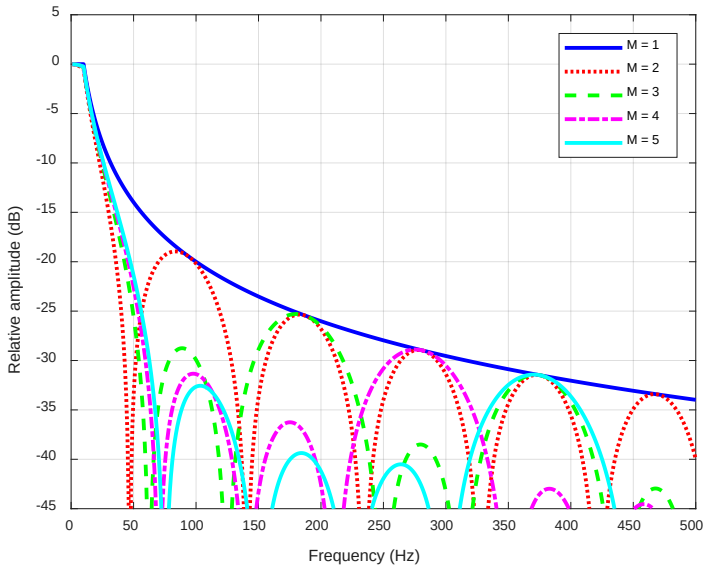

Figure 6: As for Fig. 4., but including a 20 dB per decade roll-off in the source spectrum above 10 Hz, and plotted against frequency for $\theta = 90°$.

Although still based on a simplistic model, Fig. 6 provides a good framework for understanding the cross-line (Y direction) output of any airgun array that has similar subarrays, which includes the vast majority of commercial airgun arrays. This is because the far-field output of the array in the Y direction depends only on the Y coordinates of the sources, and as all the airguns in a subarray have a similar Y coordinate, each subarray can be treated as a single source with a spectrum determined by its particular combination of airguns. If the subarrays are identical then the results presented above for a line array of identical sources apply directly. The subarrays of the array shown in Fig. 1. are not identical, but their outputs are likely to be similar enough that approximating each subarray as a single source with the same output spectrum as the other subarrays will provide useful insight. With this in mind, it is apparent from Fig. 6 that in the cross-line direction an array with two subarrays will produce a first grating lobe about 6 dB higher than an array with the same overall output, but three subarrays, which will in turn be about 4 dB higher than for an array with four subarrays. This difference may seem insignificant given that Fig. 6 shows that even for the two subarray case, the first grating lobe is 18 dB down on the array output at 10 Hz. However, as will be explained later, for near horizontal propagation, interference effects selectively filter out low frequencies, which greatly increases the importance of the grating lobes.

The same analysis can be applied to the in-line (X) direction, although in this case the big differences in airgun sizes along a typical subarray make the assumption that all sources produce the same output spectrum a much poorer approximation. Taken at face value, the relatively small spacing between airguns in the X direction would be expected to push the first grating lobe to a high enough frequency that it is of little significance due to the roll-off of the spectrum. For example, for the array shown in Fig. 1, which has an average airgun spacing in the X direction of about 2.3 m, the first grating lobe in the X direction would be expected to be at about 650 Hz. However, the fact that a large proportion of the acoustic energy is coming from the large airguns at either end of the subarrays is likely to result in a peak resembling a grating lobe at a frequency based on the overall length of the array, which in this case would be 107 Hz.

3.2 Regular planar arrays

The coordinates of the sources in a horizontal, planar array consisting of a number of identical subarrays, each aligned parallel to the X axis, can be written in the form: $(x_m, y_m, z_m) = (x_l, y_n, z_0)$, where l is the index of the source along the subarray, n is the index of the subarray, and z_0 is the array depth. In this case the source spectrum can be written as the product of a term that depends only on x_m and a term that depends only on y_m, therfore $p_{0,m}(\omega) = p_{x,l}(\omega)\, p_{y,n}(\omega)$, and Equation (5) can be factored to give:

$$p_0(\omega) \approx e^{-ikz_0\hat{z}} \sum_{l=1}^{L} p_{x,l}(\omega)\, e^{-ikx_l\hat{x}} \sum_{n=1}^{N} p_{y,n}(\omega)\, e^{-iky_n\hat{y}} \tag{7}$$

(For identical subarrays, $p_{y,n}(\omega)$ is independent of y, and therefore n, but the y dependence is retained here to keep the result more general and to make the symmetry of the equation more apparent.)

Comparing Equation (7) with Equation (6), the first summation can be recognised as the far-field output of a line array oriented in the X direction that corresponds to a single subarray, and the second summation as the response of a line array oriented in the Y direction that corresponds to the array made up of subarrays discussed in the previous section. The overall response is simply the product of these two line array responses and a phase term dependent on the depth of the array.

The horizontal-plane output of a planar array consisting of three parallel strings of seven identical sources, each with a 20 dB per decade spectral roll-off above 10 Hz is plotted on the left side of Fig. 7. Sources in each string are spaced by 2.333 m in the X direction and adjacent strings are spaced by 8 m in the Y direction. This is a similar geometry to the array shown in Fig. 1. Note that in Fig. 7, the variation in relative amplitude along the 90° radial is determined by the number and spacing of subarrays, and corresponds exactly to the 3 source line array case plotted in Fig. 6.

The output of the array shown in Fig. 1 was calculated using CMST's airgun array model, Cagam (which is based on Johnson (1994)), and is plotted on the right in Fig. 7 for comparison with the simple model. Despite the many approximations involved in the simple model, there is a very close correspondence between the two plots in the cross-line (Y) direction. In the in-line (X) direction, the simple model under-predicts the relative amplitudes of the sidelobes (a consequence of assuming all sources have the same output spectrum), but the positions of the sidelobes correspond quite closely.

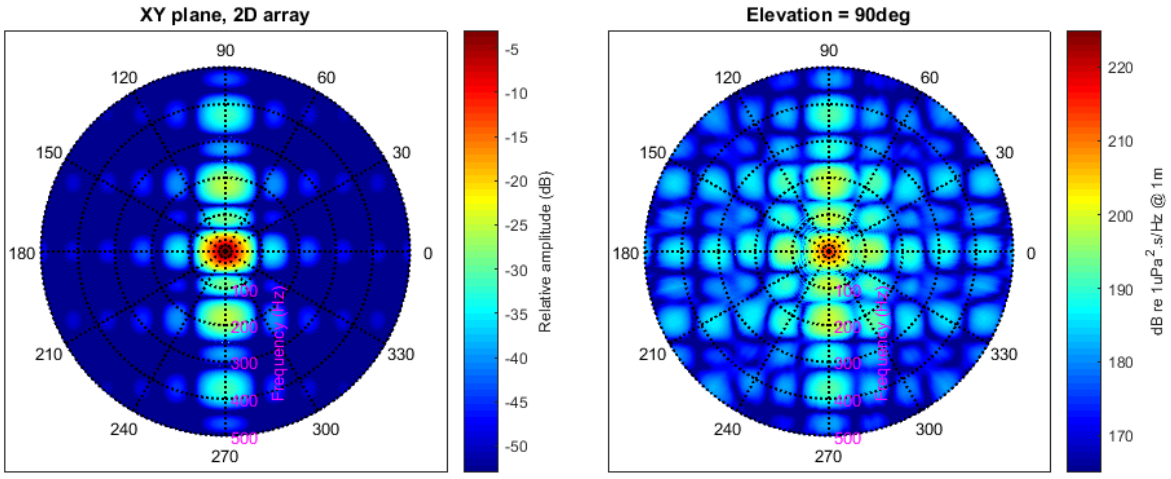

Figure 7: Left: horizontal-plane far-field output ($20\log_{10}|p_0|$) plotted as a function of both frequency (radial coordinate) and angle from the X-axis for a horizontal planar array consisting of three parallel strings of seven identical sources, each with a 20 dB per decade spectral roll-off above 10 Hz. Sources in each string are spaced by 2.333 m in the X direction and adjacent strings are spaced by 8 m in the Y direction. Right: horizontal-plane far-field output of the array shown in Fig. 1 calculated using the Cagam airgun array model.

3.3 Effect of sea surface reflections

Airgun arrays are usually towed close to the sea surface, with typical depths ranging between 4 m and 10 m. This is partly to simplify the logistics of providing a continuous supply of compressed air to the airguns and partly to provide a combined direct and surface reflected signal with desirable characteristics in the vertically downward direction.

Due to the fact that the acoustic impedance of air is much lower than that of water, the sea surface is effectively a pressure-release boundary for underwater sound, and so acoustic signals incident on the sea surface from below are inverted on reflection. Direct and surface-reflected signals therefore tend to destructively interfere with the consequent attenuation increasing as the time delay between the two arrivals, relative to the period of the signal, decreases. This effect acts as a high-pass filter; attenuating low frequency signals more than high frequency signals, and becomes increasingly pronounced as the elevation angle approaches the horizontal, which corresponds to the directions most important for long range propagation in the ocean. The resulting high-pass filtering effect is illustrated in the left-hand plot in Fig. 8, which can be compared to the right-hand plot in Fig. 7 and shows that, when the surface reflection is included, the relative importance of the array output at frequencies below 100 Hz is much reduced. In this particular case, the highest output now occurs at the first grating lobe in the cross-line (Y) direction which, as discussed above, is determined by the spacing between subarrays.

Integrating the array output energy over frequency and converting to dB provides an effective source sound exposure level (SEL) for each direction. Doing this for the 75° elevation output that includes the surface reflection and plotting the result against azimuth results in the blue curve in the right-hand plot in Fig. 8 which, as expected, shows that the highest output is in the cross-line (Y) direction, and is about 3 dB higher than the next highest output, which is in the in-line (X) direction.

In practice the output of the array over a range of elevation angles is important, and the interaction of sound with the seabed and other propagation effects complicate this simple picture, but more accurate modelling carried out by the author for a wide variety of arrays and scenarios shows that in the majority of cases the highest sound levels are produced in the cross-line direction, and that this is largely due to the first grating lobe. For this array, the next most significant output is the first sidelobe in the in-line (X) direction which, as discussed in Section 3.1, is a result of large airguns being placed at either end of the subarrays.

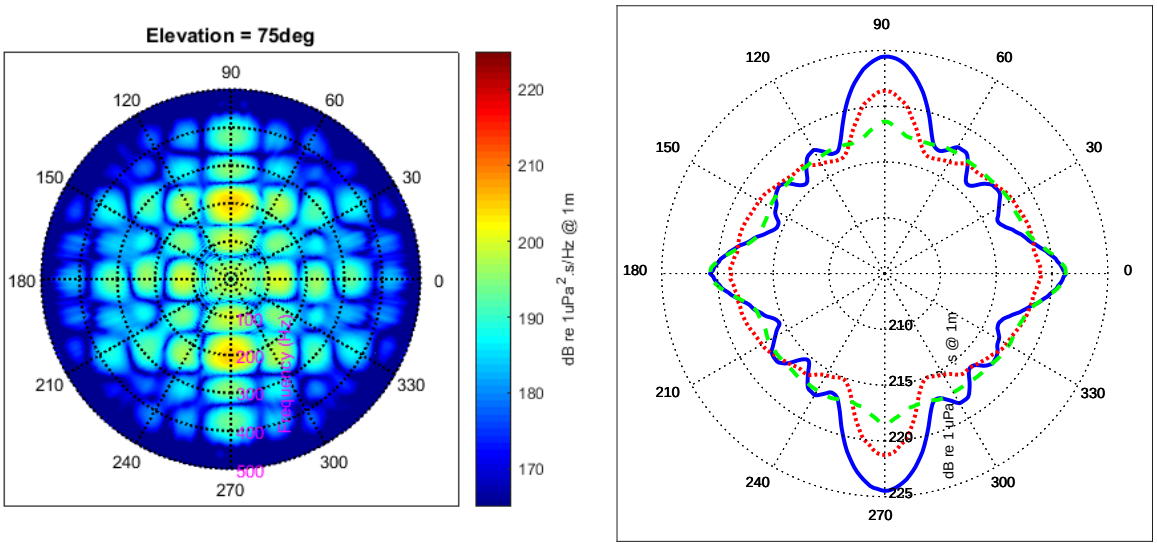

Figure 8: Left: Far-field output of the array shown in Fig. 1 modelled by Cagam for an elevation angle of 75° from the vertical (corresponding to 15° from the horizontal), including the effect of the surface reflection. Right: Corresponding effective source sound exposure level as a function of azimuth for the same array (blue), and for the four-subarray (red dotted) and five-subarray (green broken) arrays shown in Fig. 9.

4 IMPLICATIONS FOR ARRAY DESIGN

The results presented above lead to two simple principles for minimising the near-horizontal output of an airgun array:

1. Increase the number of subarrays to minimise their spacing. This will increase the frequency of the first grating lobe in the cross-line direction, which will reduce its amplitude due to the high-frequency roll-off of the airgun spectrum.

2. Concentrate the large airguns in the centre of the array. This will reduce the amplitude of the first sidelobe.

There are, of course, constraints due to the requirement to maintain the array's performance for its primary purpose as a seismic survey source, and practical issues to do with deployment and operation, however it seems that relatively straightforward changes to current practice could make a useful difference. For example, Fig. 9 shows two variations of the array shown in Fig. 1, both of which use the same numbers and sizes of individual airguns and clusters as the original array, and maintain the same overall dimensions. These arrays would therefore be expected to produce signals very similar to those of the original array at the near-vertical angles important for seismic surveying, although the concentration of large airguns in the centre of the array would broaden the vertical beam somewhat.

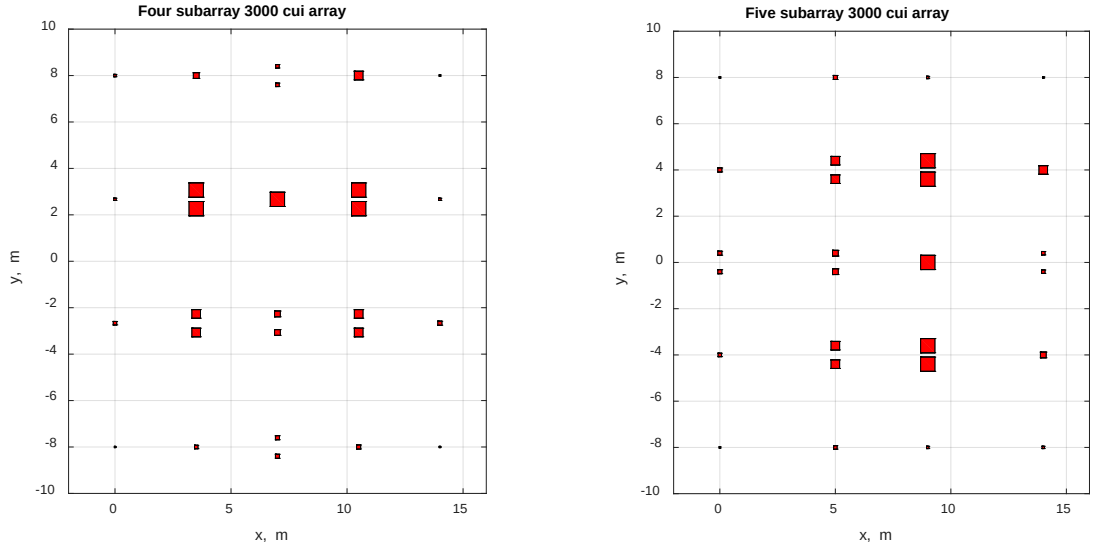

Figure 9: Four subarray (left) and five subarray (right) rearrangements of the array shown in Fig. 1.

As shown in the right-hand plot in Fig. 8, the four subarray layout would be expected to reduce SELs in the cross-line direction by about 3 dB and those in the in-line direction by about 2 dB compared to the original configuration. The five subarray version would be expected to reduce the cross-line SELs by approximately 6 dB but does not reduce the in-line levels. These configurations were arrived at by an ad hoc application of the two principles stated above, and it is possible that further improvements could be made with some additional effort.

5 CONCLUSIONS

This paper has demonstrated that many of the features of the near horizontal-plane output of airgun arrays can be explained by considering the characteristics of linear arrays of small numbers of sources. This leads to some simple principles that can be used to reduce the high output levels that typically occur in the cross-line direction at the cost of increasing the number of subarrays and rearranging the airguns within subarrays. Although the achieved reductions in levels may seem small, it should be remembered that a reduction in level of 3 dB is likely to decrease the range at which a particular SEL threshold is reached by a factor of somewhere between 1.41 (spherical spreading) and 2 (cylindrical spreading), depending on the propagation conditions.

In practice, before such changes are implemented, further analyses would be required to ensure that the modified arrays are still fit for purpose as seismic survey sources, and the implications of the changes for array deployment equipment and procedures would need to be assessed.

REFERENCES

Compton, R., Goodwin, L., Handy, R., Abbott, V. (2008). ”A critical examination of worldwide guidelines for minimising the disturbance to marine mammals during seismic surveys”. Marine Policy, 32(3), 255-262.

Duncan, A.J., Weilgart, L. S., Leaper, R., Jasny, M., Livermore, S., "A modelling comparison between received sound levels produced by a marine vibroseis array and those from an airgun for some typical seismic scenarios", Marine Pollution Bulletin (2017), http://dx.doi.org/10.1016/j.marpolbul.2017.04.001

Gisiner, R. C. (2016), “Sound and marine seismic surveys”, Acoustics Today, 12 (4), Winter 2016, pp. 10-18.

Johnson, D. T. (1994). "Understanding airgun bubble behaviour". Geophysics, 59(11), 1729-1734

Kinsler, L. E., Frey, A. R., Coppens, A. B., Sanders, J. V. (2000). *Fundamentals of acoustics*, 4th ed., John Wiley & Sons, ISBN 978-0-471-84789-2.

LGL and MAI. (2011). "Environmental Assessment of Marine Vibroseis." LGL Rep. TA4604-1; JIP contract 22 07-12. Rep. from LGL Ltd., environ. res. assoc., King City, Ont., Canada, and Marine Acoustics Inc., Arlington, VA, U.S.A., for Joint Industry Programme, E&P Sound and Marine Life, Intern. Assoc. of Oil & Gas Producers, London, U.K. 207 p.

McCauley, R. D., Day, R. D., Swadling, K. M., Fitzgibbon, Q. P., Watson, R. A., and Semmens, J. M. (2017). “Widely used marine seismic survey air gun operations negatively impact zooplankton.” Nature Ecology & Evolution, 1, 0195, doi: 10.1038/s41559-017-0195.

McCauley, R. D., Fewtrell, J., and Popper, A. N. (2003). “High intensity anthropogenic sound damages fish ears”. Journal of the Acoustical Society of America, 113, 638–642.

Parkes, G. E. and Hatton, L. (1986), The Marine Seismic Source, Springer, ISBN 978-94-017-3385-4.

PGS (2005), "PGS Electrical marine Vibrator", PGS Tech Link, Vol. 5, No. 11, November 2005. Available from: www.pgs.com/GeophysicalServices/Technical_Library/TechLink_Articles/TechLink_November_2005/PGS_Electrical_Marine_Vibrator/

Pramik, B. (2013). “Marine Vibroseis: shaking up the industry”. first break, 31, 67-72.

Southall, B. L., et. al. (2007), “Marine mammal noise exposure criteria: initial scientific recommendations”. *Aquatic Mammals*, 33 (4), 411-522.

Tenghamn, R. (2006). “An electrical marine vibrator with a flextensional shell”. Exploration Geophysics, 37, 286-291.